

Compact triplexer in two-dimensional hexagonal lattice photonic crystals

Hongliang Ren (任宏亮)^{1*}, Jianping Ma (马建平)², Hao Wen (温浩)¹, Yali Qin (覃亚丽)¹, Zhefu Wu (吴哲夫)¹, Weisheng Hu (胡卫生)³, Chun Jiang (姜淳)³, and Yaohui Jin (金耀辉)³

¹College of Information Engineering, Zhejiang University of Technology, Hangzhou 310023, China

²College of Computer Science and Technology, Zhejiang University of Technology, Hangzhou 310023, China

³State Key Laboratory of Advanced Optical Communication Systems and Networks, Shanghai Jiao Tong University, Shanghai 200240, China

*Corresponding author: hlren@zjut.edu.cn

Received October 18, 2010; accepted December 7, 2010; posted online March 15, 2011

We design a compact triplexer based on two-dimensional (2D) hexagonal lattice photonic crystals (PCs). A folded directional coupler (FDC) is introduced in the triplexer beside the point-defect micro-cavities and line-defect waveguides. Because of the reflection feedback of the FDC, high channel drop efficiency can be realized and a compact size with the order of micrometers can be maintained. The proposed device is analyzed using the plane wave expansion method, and its transmission characteristics are calculated using the finite-difference time-domain method. The footprint of the triplexer is about $12 \times 9 \mu\text{m}$, and its extinction ratios are less than -20 dB for 1310 nm, approximately -20 dB for 1490 nm, and under -40 dB for 1550 nm, making it a potentially essential device in future fiber-to-the-home networks.

OCIS codes: 250.5300, 230.5750, 230.7370.

doi: 10.3788/COL201109.042501.

The fiber-to-the-home (FTTH) system has been deemed a promising solution for broadband access networks, in which an optical triplexer plays a highly important role^[1,2]. Three wavelength channels are designed in the filter device, i.e., 1310 nm for the up-stream signal, as well as 1490 and 1550 nm for the down-stream signals according to ITU G.983 recommendations. Conventional optical triplexers are currently mostly fabricated using a planar lightwave circuit and arrayed waveguide grating technology^[1-5]. The former is the most promising candidate for low-cost devices, and has been developed commercially. The latter is the most commonly used planar waveguide device in dense and coarse wavelength-division-multiplexing (WDM) communication systems. These traditional technologies present numerous considerable advantages, such as high performance, high reliability, and easy integration.

However, these conventional devices are disadvantageous in terms of their large size, which is about the order of millimeters to centimeters. Consequently, it is gradually becoming unsuitable for the demands of integrated optoelectronic devices. Based on two-dimensional (2D) photonic crystals (PCs) with artificial periodic structures, even smaller devices can be fabricated^[6-8]. Thus far, many researchers have designed these devices in PCs^[9-18], and the disadvantage presented by the large device footprint can be overcome, indicating that high density optical integration can be realized. Using a point-defect micro-cavity in PCs with a square lattice, the triplexers were engineered with compact sizes and high efficiency by Shih *et al.*^[19] Moreover, Park *et al.* proposed a triplexer based on the square lattice PCs; these have smaller sizes than that presented by Shih *et al.*^[20,21] Shi *et al.* also put forward a triplexer by cascading two stages of directional couplers based on a PC with

a hexagonal lattice of dielectric rods in air^[22]. Considering fabrication technology, however, it is easier to make triplexers based on hexagonal lattice PCs with the air holes perforated in a high dielectric refractive index slab compared with the PCs with high dielectric refractive index rods in air.

Recently, a three-port channel drop filter with a folded directional coupler (FDC) has been proposed based on 2D PCs; compact sizes and high drop efficiency are realized through the directional coupler^[23]. In this letter, a FDC is used to design a new triplexer based on hexagonal lattice PCs with the air holes perforated in a high dielectric refractive index slab. In the structure, the FDC is elaborately engineered to filter a wavelength signal of 1310 nm with high efficiency using the

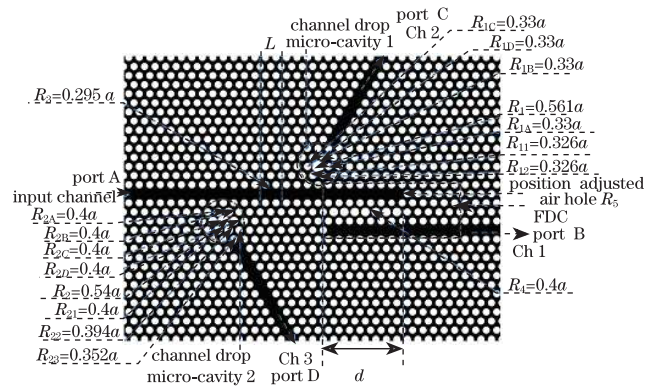


Fig. 1. Structure of the proposed triplexer. The radius of the PC air holes is $r = 0.33a$, where a is the lattice constant. In the bus waveguide section between the two micro-cavities, the waveguide propagation constant is changed to meet the phase term, and the radius of border air holes in the waveguide section is $R_3 = 0.295a$.

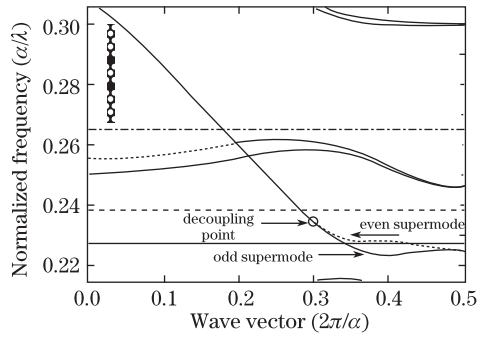


Fig. 2. Dispersion curves for the two-waveguide modes of the FDC. The operational frequencies of the triplexer are denoted by the solid, dashed, and dot-dashed lines, and the normalized frequencies are $0.22614(a/\lambda)$, $0.23525(a/\lambda)$, and $0.26757(a/\lambda)$, respectively, whose corresponding wavelengths are 1550, 1490, and 1310 nm, respectively, for the lattice constant of 350.5 nm. The inset shows the supercell of the calculated W1 PC waveguide (W1 means one row of holes).

directional coupler function, and the wavelength signals of 1490 and 1550 nm as the down-stream signals are dropped with high channel drop efficiency because of the reflection feedback of the FDC.

For 2D PCs with a hexagonal lattice of air holes in GaAs (dielectric constant $\varepsilon = 11.6964$), the chosen radius of background air holes is $r = 0.33a$, where $a = 350.5$ nm represents the lattice constant. The structure is simulated by plane wave expansion (PWE) and has a photonic bandgap (PBG) for transverse-electric modes, which have no electric field in the direction of propagation. The PBG extends from $0.22278(a/\lambda)$ to $0.31392(a/\lambda)$, where λ is the wavelength of light in free space. The triplexer is engineered based on the PCs with the hexagonal lattice of air holes in GaAs, and its structure is depicted in Fig. 1. One horizontal row of air holes is removed as the input channel waveguide, and channels 1 and 2 waveguides are obtained as channel drop waveguides by removing the air holes located along the orientation wherein the ΓK direction turns

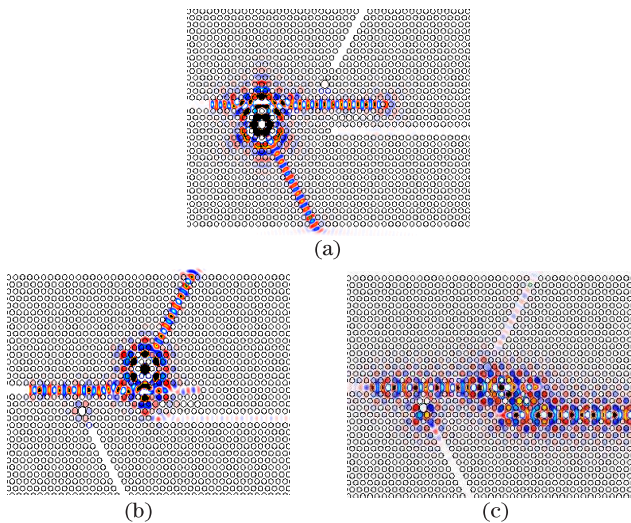


Fig. 3. Steady-state electric field distributions of optical triplexer for the three wavelength signals of (a) 1310 nm, (b) 1490 nm, and (c) 1550 nm.

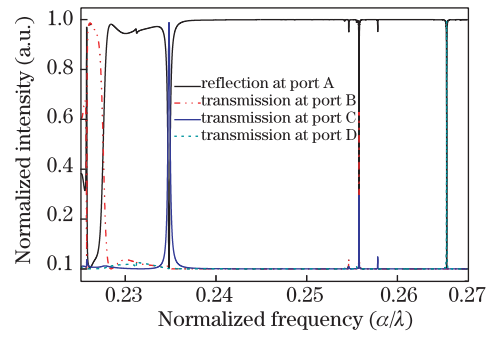


Fig. 4. Frequency response of the triplexer at $s = 0.15a$ calculated using the FDTD method.

anti-clockwise by 60° and 300° . Channel drop micro-cavities 1 and 2 relate the input channel waveguide to channels 1 and 2, respectively (Fig. 1). Micro-cavity 1 is designed to drop a wavelength signal of 1490 nm, and its normalized resonant frequency is $0.23525(a/\lambda)$. Figure 1 shows that in micro-cavity 1, the radius of central air hole R_1 increases to $0.561a$, and the radius of the nearest two air holes surrounding the central air hole decreases to $R_{11} = R_{12} = 0.326a$, whereas the radii of the other four nearest air holes adjacent to the central large air hole are $R_{1A} = R_{1B} = R_{1C} = R_{1D} = 0.33a$. The normalized resonant frequency of micro-cavity 2 is $0.26757(a/\lambda)$, and it filters a wavelength signal of 1310 nm. In the structure of micro-cavity 2, the radius of central air hole R_2 increases to $0.54a$, and the radii of the two nearest air holes adjacent to the central large air hole are added to $R_{21} = 0.4a$ and $R_{22} = 0.394a$, respectively. The radii of the other four nearest air holes surrounding the central large air hole are $R_{2A} = R_{2B} = R_{2C} = R_{2D} = 0.4a$. In addition, the radius of the air hole between micro-cavity 2 and channel 2 increases to $R_{23} = 0.352a$ to elaborately adjust the resonant frequency of the micro-cavity. To improve the channel drop efficiency and filter a third wavelength signal of 1550 nm, a FDC is introduced to connect ports A and B (Fig. 1).

Firstly, using the FDC, the triplexer is designed to filter a wavelength signal of 1550 nm. The FDC is cascaded between port A of the input channel waveguide and output port B, and it is composed of two parallel and identical PC waveguides with a coupling distance of $d=8a$, in which the PC waveguides are also obtained by removing the air holes in the ΓK direction. In Fig. 1, two waveguides of the FDC are separated by three rows of air holes, and the radius of the central row of air holes increases to $R_4 = 0.4a$. Compared with a point-defect micro-cavity side-coupled to the line-defect waveguide, the FDC also exhibits a resonant notch-rejection transmission behavior when a resonance condition is satisfied^[24,25]. In the coupler region of the FDC, the dispersion relations (Fig. 2) are calculated using the PWE method; the inset of Fig. 2 shows the calculated supercell of the coupler region. In Fig. 2, the normalized frequency at the decoupling point is $f_D = 0.235(a/\lambda)$, and the fundamental modes of two individual waveguides are split into even and odd super-modes at $f < f_D$. When the fundamental modes of two waveguides are non-separate at certain frequencies, the light is completely reflected back as it passes

through the FDC. While the fundamental modes are divided, the corresponding propagating constants of even and odd super-modes are denoted by β_e and β_o , respectively, and the FDC can realize the filtering function of common PC directional couplers. At $f = 0.22614(a/\lambda)$, these propagating constants of super-modes β_o and β_e are $0.34513(2\pi/a)$ and $0.46109(2\pi/a)$, respectively, for which the frequencies are denoted by the solid line in Fig. 2. Then, the coupling length L_c is $8.6a$ according to formula $L_c = \pi/(\beta_e - \beta_o)$, where the value is nearly equal to coupling distance d . At normalized frequency, the light can completely pass through the FDC, and the corresponding wavelength is 1550 nm. For $f = 0.23525(a/\lambda)$ and $f = 0.26757(a/\lambda)$, both frequencies are larger than that at the decoupling point, and the two frequencies are denoted by the dashed and dot-dashed lines, respectively, in Fig. 2. The waveguides demonstrate a single mode at two frequencies, and their corresponding wavelengths are 1490 and 1310 nm, respectively. Because no split occurs between two individual fundamental modes, the wavelength signal of 1310 or 1490 nm is completely reflected to the input port when it propagates through the FDC. Subsequently, the channel drop efficiencies are enhanced in channels 1 and 2 when the reflection feedback phase matching conditions are satisfied^[12].

Secondly, achieving high channel drop efficiency for a wavelength signal of 1490 nm is a favorable approach. According to previous theoretic work, the distance L from the resonator to the FDC is set for the phase matching conditions $\beta L = m\pi + \pi/2$, where β is the propagation constant of the waveguide mode at the frequency, and m is an integer^[12,20]. To make the device compact, the distance between the left end of the FDC and the central large air hole of micro-cavity 1 is $0.5a$. Unfortunately, numerical results calculated by the finite-difference time-domain (FDTD) methods demonstrate that the channel drop efficiency is only close to 90%, indicating that the phase matching terms are not satisfied. Here, a new method is introduced to adjust the reflection feedback phase by adjusting the position of the air holes at the right end of the upper waveguide in the FDC. The hole R_5 is located in the reflection interface as a wavelength signal of 1490 nm launched at port A propagates through the FDC. Thus, the additional reflection phase can be modified by adjusting the position of hole R_5 at the reflection interface. Then, the hole is shifted to the left with displacement $s = 0.15a$ relative to the unmodified lattice.

Finally, to realize high channel drop efficiency using the channel drop micro-cavity 2, the phase matching conditions are also required for a wavelength signal of 1310 nm. The distance between the central large air holes of micro-cavities 1 and 2 is $9a$. The large distance does not lead to the mutual disturbance of the structural parameters of the two micro-cavities, and changes in their resonant frequencies are avoided. Subsequently, the radius of border air holes adjacent to part of the input channel waveguide between micro-cavities 1 and 2 is reduced to $R_3 = 0.295a$ to meet the reflection matching conditions by adjusting the dispersion relationships of this section of input channel waveguide, where its length L' is $2a$. The shortest distance between these adjusted air holes and the central large air hole of micro-cavity

1 or 2 is $4a$, which avoids changes in the resonator frequency.

The function of the triplexer was simulated using the 2D FDTD method. Figure 3 shows the steady-state electric fields for the three wavelength signals of 1310, 1490, and 1550 nm. From it, we prove that the triplexer can efficiently divide the three mixed wavelength signals. As port A was used as a common input port for this simulation, a wavelength signal of 1310 nm was input at port D in the actual application of the device and port A became the output port for up-stream operation. Because reciprocity is satisfied in the proposed device, however, its propagation characteristics are independent of the propagation direction of the signal.

Figure 4 shows the frequency response of the triplexer calculated by FDTD, in which the Gaussian light pulse is launched at port A, and the reflection spectrum at port A and transmission spectra at ports B, C, and D are depicted by thick solid, dot-dashed, thin solid, and dashed lines, respectively. Because of the incorporation of the FDC as a frequency-dependent reflective mirror, the channel drop efficiencies for the wavelength signals of 1310, 1490, and 1550 nm are all more than 98.5%. Although the filter bandwidths at the three wavelengths are different and some energy drop at other certain frequencies is obtained, the device can be very convenient and useful in a FTTH communication system, where only three mixed wavelength signals are considered.

The transmission performance of the triplexer is quantitatively obtained by calculating an extinction ratio, which is defined as the ratio of the power at the output port desired for a specific wavelength to the power at an undesired port. The crosstalk characteristics of the device are shown in Table 1, and the crosstalk range is between -19.69 and -42.92 dB. We confirm that the triplexer performs satisfactorily in practical applications.

In conclusion, we present a novel design of a triplexer based on 2D hexagonal lattice PCs with air holes perforated in high dielectric slabs. A FDC is incorporated to enhance the channel drop efficiency and make the device compact. The optical filter for a wavelength signal of 1310 nm is obtained by the directional coupler function of the FDC. The two other wavelength signals, 1490 and 1550 nm, are dropped with high channel drop efficiency because of the reflection feedback of the FDC. The size of the optical triplexer is about $35a \times 26a$ and its actual size is 12×9 (μm) for a lattice of 350.5 nm. In the practical triplexer, considering the vertical confinement of photons is necessary, and the design of three-dimensional (3D) PCs-based triplexer requires extension.

This work was supported by the National Natural Science Foundation of China (Nos. 60978010, 60907032, and 60825103), the Natural Science Foundation of Zhejiang Province (No. Y1090169), the Foundation of Zhejiang

Table 1. Crosstalk Characteristics

Channel	1	2	3
1 (1550 nm)	–	–21.03 dB	–21.67 dB
2 (1490 nm)	–19.69 dB	–	–30.36 dB
3 (1310 nm)	–42.92 dB	–42.92 dB	–

University of Technology (No. 0901103012408), and the Open Fund of the State Key Laboratory of Advanced Optical Communication Systems and Networks, China (No. 2008sh07).

References

1. X. Li, G.-R. Zhou, N.-N. Feng, and W. Huang, *IEEE Photon. Technol. Lett.* **17**, 1214 (2005).
2. T. Lang, J.-J. He, and S. He, *IEEE Photon. Technol. Lett.* **18**, 232 (2006).
3. C. R. Doerr, M. Cappuzzo, L. Gomez, E. Chen, A. Wong-Foy, C. Ho, J. Lam, and K. McGreer, *J. Lightwave Technol.* **23**, 62 (2005).
4. M. K. Smit and C. van Dam, *IEEE J. Sel. Top. Quantum Electron.* **2**, 236 (1996).
5. Y. Inoue, T. Oguchi, Y. Hibino, S. Suzuki, M. Yanagisawa, K. Moriwaki, and Y. Yamada, *Electron. Lett.* **32**, 847 (1996).
6. E. Yablonovitch, *Phys. Rev. Lett.* **58**, 2059 (1987).
7. S. John, *Phys. Rev. Lett.* **58**, 2486 (1987).
8. K. Sakoda, *Optical Properties of Photonic Crystals* (Springer, New York, 2004).
9. S. Noda, K. Tomoda, N. Yamamoto, and A. Chutinan, *Science* **289**, 604 (2000).
10. S. Fan, P. R. Villeneuve, J. D. Joannopoulos, and H. A. Haus, *Phys. Rev. Lett.* **80**, 960 (1998).
11. C. Manolatou, M. J. Khan, S. Fan, P. R. Villeneuve, H. A. Haus, and J. D. Joannopoulos, *IEEE J. Quantum Electron.* **35**, 1322 (1999).
12. S. Kim, I. Park, H. Lim, and C.-S. Kee, *Opt. Express* **12**, 5518 (2004).
13. H. Takano, B.-S. Song, T. Asano, and S. Noda, *Opt. Express* **14**, 3491 (2006).
14. C. Ren, J. Tian, S. Feng, H. Tao, Y. Liu, K. Ren, Z. Li, B. Cheng, D. Zhang, and H. Yang, *Opt. Express* **14**, 10014 (2006).
15. S. Chen, P. Hu, T. Yu, Q. Liao, and Y. Huang, *Acta Photon. Sin.* (in Chinese) **38**, 2588 (2009).
16. H. Wang, K. Li, F. Kong, L. Song, and L. Mei, *Acta Photon. Sin.* (in Chinese) **37**, 1122 (2008).
17. H. Ren, C. Jiang, W. Hu, M. Gao, and J. Wang, *Opt. Express* **14**, 2446 (2006).
18. H. Ren, Y. Qin, K. Liu, Z. Wu, W. Hu, C. Jiang, and Y. Jin, *Chin. Opt. Lett.* **8**, 749 (2010).
19. T.-T. Shih, Y.-D. Wu, and J.-J. Lee, *IEEE Photon. Technol. Lett.* **21**, 18 (2009).
20. D.-S. Park, J.-H. Kim, B.-H. O, S.-G. Park, E.-H. Lee, and S. G. Lee, *Proc. SPIE* **6989**, 69891S (2008).
21. D.-S. Park, B.-H. O, S.-G. Park, E.-H. Lee, and S. G. Lee, *Proc. SPIE* **6897**, 689711 (2008).
22. Y. Shi, D. Dai, and S. He, *IEEE Photon. Technol. Lett.* **18**, 2293 (2006).
23. C.-C. Wang and L.-W. Chen, *Physica B* **405**, 1210 (2010).
24. T. P. White, L. C. Botten, R. C. McPhedran, and C. M. de Sterke, *Opt. Lett.* **28**, 2452 (2003).
25. T. P. White, L. C. Botten, C. M. de Sterke, R. C. McPhedran, A. A. Asatryan, and T. N. Langtry, *Phys. Rev. E* **70**, 056607 (2004).